Progress In Electromagnetics Research, Vol. 136, 543–559, 2013

ANALYSIS OF TRANSIENT ELECTROMAGNETIC SCATTERING USING TIME DOMAIN FAST DIPOLE METHOD

Ji Ding*, Changqing Gu, Zhuo Li, and Zhenyi Niu

College of Electronic and Information Engineering, Nanjing University of Aeronautics and Astronautics, Nanjing 210016, China

Abstract—In this paper, a new time domain fast dipole method (TD-FDM) is proposed for solving time-domain magnetic field integral equations. The proposed scheme is the extension of the frequency domain fast dipole method (FDM) to the time domain. The principle is based on the Taylor series expansion of far fields. The computational complexity of TD-FDM scales as $O(N_s^{3/2}N_t)$ as opposed to $O(N_s^2N_t)$ for marching-on in-time (MOT) method. Here, N_s is the number of spatial basis functions and N_t is the number of the time steps. Numerical results about the electromagnetic scattering from perfect electric conductor (PEC) objects are given to demonstrate the validity and efficiency of the proposed scheme.

1. INTRODUCTION

Time-domain integral-equation (TDIE) [1–6] methods have enjoyed widespread engineering applications, especially the analysis of broadband electromagnetic scattering. When analyzing the scattering from perfect electric conductor (PEC), the TDIE methods require a discretization of the scatterer surface and do not call for absorbing boundary conditions in the finite difference time domain [7, 8]. However, with the electrical size of the scatterer increasing, the memory requirement and the computational complexity become very expensive. The computational complexity of classical marching-on in-time (MOT) scheme for solving TDIE scales as $O(N_s^2N_t)$.

In the past decades, many fast algorithms have been presented to reduce the memory requirement and the computational complexity of the TDIE method. The two most famous schemes are the plane wave

Received 11 December 2012, Accepted 9 January 2013, Scheduled 23 January 2013
* Corresponding author: Ji Ding (dingji@nuaa.edu.cn).

time domain (PWTD) algorithm [9–11] and time domain adaptive integral equation method (TD-AIM) [12, 13]. The PWTD algorithm derives from the fast multipole method (FMM) [14, 15]. It relies on a Whittaker-type expansion of transient fields and decomposes radiated fields into transient plane waves. The PWTD algorithm has a computational complexity of $O(N_s^{3/2}\log(N_s)N_t)$. The TD-AIM is the extension of the frequency-domain adaptive integral method (AIM) to the time domain. It projects the source onto a uniform auxiliary grid that enclosed the scatterer and the projection matrices are block-Toeplitz on four levels. Therefore, TD-AIM can accelerate matrix-vector products via space-time fast Fourier transforms (FFTs). Like AIM, the TD-AIM scheme is less efficient than the PWTD method for solving three-dimensional surfaces structure [12].

Recently, the time domain equivalent dipole moment (TD-EDM) method [16] has been proposed to speed up the computation of impedance matrix. The surface current distribution containing two adjacent triangles is replaced by an infinitely small dipole with an equivalent dipole moment. Therefore, the TD-EDM method does not require evaluating the usual double integrals in the conventional TDIE method. Unfortunately, the TD-EDM method can not reduce matrix-vector product operations and the memory requirement. The computational complexity is still $O(N_s^2 N_t)$.

In this paper, a time domain fast dipole method (TD-FDM) is proposed for solving the electromagnetic scattering from PEC targets. The proposed scheme builds upon the authors' previous work TD-EDM reported in [16]. It is the extension of the frequency domain fast dipole method (FDM) [17–19] to the time domain. Similar to FDM, the TD-FDM starts by grouping, the spatial basis functions into geometrically equal-sized groups. If two groups are far-field group pair, the transient field can be expanded through the Taylor series and reconstructed via aggregation-translation-disaggregation procedure. It can reduce the computational complexity to $O(N_s^{3/2}N_t)$. The TD-FDM is relatively easy to implement, and efficient enough to solve many practical problems. In this paper, we focus on magnetic field integral equations (MFIE) to analyze the electromagnetic scattering, because the condition numbers of MFIE are superior to electric field integral equations (EFIE), and MFIE does not have the low frequency breakdown problem [20].

This paper is organized as follows. Section 2 describes the TD-EDM method for solving time domain integral equation. Section 3 introduces the TD-FDM scheme and explores its theoretical computational complexity and memory requirement. Section 4 gives several numerical results to demonstrate the validity of the proposed

method which is followed by our conclusions.

2. BASIC PRINCIPLE OF THE TD-EDM METHOD

Consider a closed perfect electric conductor (PEC) with surface S which resides in free space. A transient electromagnetic field is incident on the object and this field will induce a surface current $\mathbf{J}(\mathbf{r},t)$ on S that generates a scattered field. Enforcing the boundary conditions on the surface of the conductors, the time-domain MFIE formulation is obtained

$$\hat{\mathbf{n}} \times [\mathbf{H}^i(\mathbf{r},t) + \mathbf{H}^s(\mathbf{r},t)] = \mathbf{J}(\mathbf{r},t), \tag{1}$$

where $\hat{\mathbf{n}}$ represents the outward normal vector to S. The surface current density $\mathbf{J}(\mathbf{r},t)$ can be approximately expanded as

$$\mathbf{J}(\mathbf{r},t) = \sum_{n=1}^{N_s} \mathbf{f}_n(\mathbf{r}) I_n(t) = \sum_{n=1}^{N_s} \mathbf{f}_n(\mathbf{r}) \sum_{j=1}^{N_t} I_{n,j} T_j(t). \tag{2}$$

Here, $\mathbf{f}_n(\mathbf{r})$ is the RWG basis functions, $T_j(t) = T(t - j\Delta t)$ (Δt is the time step size) the temporal basis function, and $I_{n,j}$ the unknown expansion coefficient.

As shown in Fig. 1, each RWG common edge contains two inner adjacent triangles. If the electric size of the triangles is sufficiently small, we can assume that the surface current distribution does not

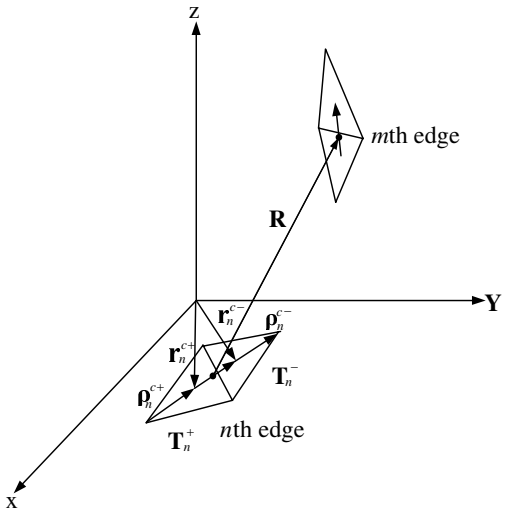

Figure 1. Configuration of the source and the testing functions.

change within the triangle. When the observation point is far away from the RWG element, each RWG element can be replaced by an infinitely small dipole having an equivalent dipole moment [21]. The dipole $\mathbf{m}_n(t)$ can be obtained by the integration of the surface current

$$\begin{aligned}\mathbf{m}_n(t) &= \int_{T_n^{\pm}} \mathbf{J}_n(\mathbf{r},t)dS = \int_{T_n^{\pm}} \mathbf{f}_n(\mathbf{r}) \sum_{j=1}^{N_t} I_{n,j}T_j(t)dS \\ &= \int_{T_n^{\pm}} \mathbf{f}_n(\mathbf{r})dS \sum_{j=1}^{N_t} I_{n,j}T_j(t) = \mathbf{m}_n \sum_{j=1}^{N_t} I_{n,j}T_j(t), \end{aligned} \tag{3}$$

where $\mathbf{m}_n = l_n(\mathbf{r}_n^{c-} - \mathbf{r}_n^{c+})$. l_n is the length of the common edge and $\mathbf{r}_n^{c\pm}$ the centers of $T_n^{\pm}$. Referring to [16] and considering Eq. (3), the radiated magnetic fields of the dipole $\mathbf{m}_n(t)$ can be expressed as

$$\mathbf{H}_n^s(\mathbf{r},t) = \frac{1}{4\pi}(\mathbf{m}_n \times \mathbf{R})\left[\frac{1}{cR^2}\sum_{j=1}^{N_t} I_{n,j}\partial_t T_j(\tau) + \frac{1}{R^3}\sum_{j=1}^{N_t} I_{n,j}T_j(\tau)\right], \tag{4}$$

where $\mathbf{R} = \mathbf{r} - \mathbf{r}'$ and $R = |\mathbf{R}|$. c is the speed of light in free space and $\tau = t - R/c$ the retarded time.

Substituting Eq. (4) into Eq. (1) and applying a spatial Galerkin testing procedure at $t_i = i\Delta t$ yields the following matrix equation

$$\mathbf{Z}_0\mathbf{I}_i = \mathbf{V}_i - \sum_{j=0}^{i-1} \mathbf{Z}_{i-j}\mathbf{I}_j, \tag{5}$$

for $0 \le i \le N_t$. The currents at all time steps can be computed recursively. The matrix element in the EDM region can be expressed as

$$[\mathbf{Z}_k]_{mn} = \frac{1}{4\pi}\mathbf{m}_m \cdot [\hat{\mathbf{n}}_m \times (\mathbf{m}_n \times \mathbf{R})]\left[\frac{1}{cR^2}\partial_t T_j(\tau) + \frac{1}{R^3}T_j(\tau)\right]\Bigg|_{t=k\Delta t}. \tag{6}$$

Note that Eq. (6) does not evaluating the surface integrals, which greatly simplifies the matrix element computation and makes matrix filling efficient.

3. TIME DOMAIN FAST DIPOLE METHOD

3.1. Implementation of the TD-FDM

From the proceeding discussion, the TD-EDM method can make the matrix filling efficient, but the drawback is that it can not accelerate the matrix-vector products of the right-hand side (RHS) of Eq. (5). The

computational bottleneck of the TD-EDM method can be alleviated with the time domain fast dipole method (TD-FDM). To apply the TD-FDM to accelerate the matrix-vector products, the scatterer must be enclosed in a fictitious cubical box and divided into several equal-sized groups. The side length of each group is D. If two groups are separated by βD ($\beta \geq 1$), we assume they are a far-field pair. Now let us consider a far-field group pair as shown in Fig. 2. The source group G_i contains the equivalent dipole $\mathbf{m}_n$ located at $\mathbf{r}_n$ and the observation group G_j contains the equivalent dipole $\mathbf{m}_m$ located at $\mathbf{r}_m$. The centers of the two groups are located at $\mathbf{r}_i$ and $\mathbf{r}_j$, respectively. The vector $\mathbf{R}$ connecting the two dipoles can be rewritten by

$$\mathbf{R} = \mathbf{r}_{mj} + \mathbf{r}_{ji} - \mathbf{r}_{ni} = \mathbf{R}_m - \mathbf{R}_n, \tag{7}$$

where $\mathbf{r}_{ji} = \mathbf{r}_j - \mathbf{r}_i$, $\mathbf{r}_{mj} = \mathbf{r}_m - \mathbf{r}_j$, $\mathbf{r}_{ni} = \mathbf{r}_n - \mathbf{r}_i$, $\mathbf{R}_m = \mathbf{r}_{mj} + \mathbf{r}_{ji}/2$, and $\mathbf{R}_n = \mathbf{r}_{ni} - \mathbf{r}_{ji}/2$. For the convenience of explanation, the dipole $\mathbf{m}_n(t)$ can be expanded as

$$\mathbf{m}_n(t) = \mathbf{m}_n \sum_{j=1}^{N_t} I_{n,j} T_j(t) = \mathbf{m}_n I_n(t). \tag{8}$$

The time signal $I_n(t)$ can be broken up into L consecutive subsignals $I_{n,l}(t)$, and each subsignal duration is $T_s = M_t \Delta t$ ($LM_t = N_t$). Thus the dipole $\mathbf{m}_n(t)$ can be rewritten as

$$\mathbf{m}_n(t) = \mathbf{m}_n \sum_{l=1}^{L} I_{n,l}(t), \tag{9}$$

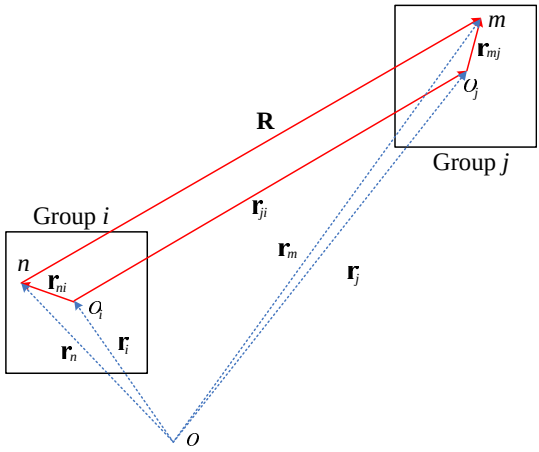

Figure 2. Configuration of a far-field group pair.

where

$$I_{n,l}(t) = \sum_{j=(l-1)M_t+1}^{lM_t} I_{n,j} T_j(t), \tag{10}$$

Then, the magnetic field $\mathbf{H}^s_{n,l}(\mathbf{r},t)$ in the observation excited by the lth time subsignal can be written as

$$\mathbf{H}^s_{n,l}(\mathbf{r},t) = \frac{1}{4\pi}(\mathbf{m}_n \times \mathbf{R}) \left[\frac{1}{cR^2}\partial_t I_{n,l}(\tau) + \frac{1}{R^3} I_{n,l}(\tau)\right]. \tag{11}$$

To further investigate TD-FDM, the inner product of $\hat{\mathbf{n}}_m \times \mathbf{H}^s_{n,l}(\mathbf{r},t)$ with the basis function can be written as

$$\begin{aligned}
&\langle \mathbf{m}_m, \hat{\mathbf{n}}_m \times \mathbf{H}^s_{n,l}(\mathbf{r},t)\rangle \\
=&\frac{1}{4\pi}\mathbf{m}_m \cdot [\hat{\mathbf{n}_m} \times (\mathbf{m}_n \times \mathbf{R})] \left[\frac{1}{cR^2}\partial_t I_{n,l}(\tau) + \frac{1}{R^3} I_{n,l}(\tau)\right] \\
=&\frac{1}{4\pi}(\mathbf{m}_m \times \hat{\mathbf{n}}_m) \cdot (\mathbf{m}_n \times \mathbf{R})\delta(\tau) * \left[\frac{1}{cR^2}\partial_t I_{n,l}(t) + \frac{1}{R^3} I_{n,l}(t)\right],
\end{aligned} \tag{12}$$

where $*$ denotes the temporal convolution. Referring to [14], we consider R in τ and expand it using the Taylor series as

$$R = |\mathbf{R}| = |\mathbf{r}_{ji} + \mathbf{r}_{mj} - \mathbf{r}_{ni}| \approx r_c + r_m + r_n, \tag{13}$$

where

$$r_m = \left[\hat{\mathbf{r}}_{ji} \cdot \mathbf{r}_{mj} + \frac{(\mathbf{r}_{mj} \cdot \mathbf{r}_{mj}) - (\hat{\mathbf{r}}_{ji} \cdot \mathbf{r}_{mj})^2}{2r_{ji}}\right], \tag{14}$$

$$r_n = \left[-\hat{\mathbf{r}}_{ji} \cdot \mathbf{r}_{ni} + \frac{(\mathbf{r}_{ni} \cdot \mathbf{r}_{ni}) - (\hat{\mathbf{r}}_{ji} \cdot \mathbf{r}_{ni})^2}{2r_{ji}}\right]. \tag{15}$$

Here, $r_c = r_{ji} = |\mathbf{r}_{ji}|$ is the distance between the two group centers and $\hat{\mathbf{r}}_{ji} = \mathbf{r}_{ji}/r_{ji}$. Consequently, substituting Eq. (13) into Eq. (12), we can obtain the following equation

$$\begin{aligned}
&\left\langle \mathbf{m}_m, \hat{\mathbf{n}}_m \times \mathbf{H}^s_{n,l}(\mathbf{r},t)\right\rangle = \frac{1}{4\pi}(\mathbf{m}_m \times \hat{\mathbf{n}}_m) \cdot (\mathbf{m}_n \times \mathbf{R})\delta(t - r_m/c) \\
&* \delta(t - r_c/c) * \delta(t - r_n/c) * \left[\frac{1}{cR^2}\partial_t I_{n,l}(t) + \frac{1}{R^3} I_{n,l}(t)\right].
\end{aligned} \tag{16}$$

For the amplitude approximation of Eq. (16), $1/R^\alpha$ for $\alpha > 0$ can also be expanded using the Taylor series as

$$\frac{1}{R^\alpha} = \frac{1}{r_{ij}^\alpha}\left[1 - \alpha\left(\frac{\hat{\mathbf{r}}_{ji} \cdot \mathbf{r}_{mj}}{r_{ij}} + \frac{\hat{\mathbf{r}}_{ij} \cdot \mathbf{r}_{ni}}{r_{ij}}\right)\right] = \frac{1}{r_{ij}^\alpha}\left[x_m^{(\alpha)} + x_n^{(\alpha)}\right], \tag{17}$$

where

$$x_m^{(\alpha)} = \frac{1}{2} - \alpha \frac{\hat{\mathbf{r}}_{ji} \cdot \mathbf{r}_{mj}}{r_{ij}}, \tag{18}$$

$$x_n^{(\alpha)} = \frac{1}{2} - \alpha \frac{\hat{\mathbf{r}}_{ij} \cdot \mathbf{r}_{ni}}{r_{ij}}. \tag{19}$$

Substituting Eq. (7) and (17) into Eq. (16), we can obtain

$$\begin{aligned}
&\langle \mathbf{m}_m, \hat{\mathbf{n}}_m \times \mathbf{H}^s_{n,l}(\mathbf{r},t) \rangle \\
&= \frac{1}{4\pi} \left\{ \left[x_m^{(3)} (\mathbf{m}'_m \times \mathbf{R}_m) \delta(\tau_m) \right]^\dagger * \left[\frac{\delta(\tau_c)}{r_c^3} \right] * [\mathbf{m}_n \delta(\tau_n)] * I_{n,l}(t) \right. \\
&\quad + \left[(\mathbf{m}'_m \times \mathbf{R}_m) \delta(\tau_m) \right]^\dagger * \left[\frac{\delta(\tau_c)}{r_c^3} \right] * \left[x_n^{(3)} \mathbf{m}_n \delta(\tau_n) \right] * I_{n,l}(t) \\
&\quad + \left[x_m^{(3)} \mathbf{m}'_m \delta(\tau_m) \right]^\dagger * \left[\frac{\delta(\tau_c)}{r_c^3} \right] * [(\mathbf{m}_n \times \mathbf{R}_n) \delta(\tau_n)] * I_{n,l}(t) \\
&\quad + \left[\mathbf{m}'_m \delta(\tau_m) \right]^\dagger * \left[\frac{\delta(\tau_c)}{r_c^3} \right] * \left[x_n^{(3)} (\mathbf{m}_n \times \mathbf{R}_n) \delta(\tau_n) \right] * I_{n,l}(t) \\
&\quad + \left[x_m^{(2)} (\mathbf{m}'_m \times \mathbf{R}_m) \delta(\tau_m) \right]^\dagger * \left[\frac{\delta(\tau_c)}{c r_c^2} \right] * [\mathbf{m}_n \delta(\tau_n)] * \partial_t I_{n,l}(t) \\
&\quad + \left[(\mathbf{m}'_m \times \mathbf{R}_m) \delta(\tau_m) \right]^\dagger * \left[\frac{\delta(\tau_c)}{c r_c^2} \right] * \left[x_n^{(2)} \mathbf{m}_n \delta(\tau_n) \right] * \partial_t I_{n,l}(t) \\
&\quad + \left[x_m^{(2)} \mathbf{m}'_m \delta(\tau_m) \right]^\dagger * \left[\frac{\delta(\tau_c)}{c r_c^2} \right] * [(\mathbf{m}_n \times \mathbf{R}_n) \delta(\tau_n)] * \partial_t I_{n,l}(t) \\
&\quad \left. + \left[\mathbf{m}'_m \delta(\tau_m) \right]^\dagger * \left[\frac{\delta(\tau_c)}{c r_c^2} \right] * \left[x_n^{(2)} (\mathbf{m}_n \times \mathbf{R}_n) \delta(\tau_n) \right] * \partial_t I_{n,l}(t) \right\},
\end{aligned} \tag{20}$$

where $\mathbf{m}'_m = \mathbf{m}_m \times \hat{\mathbf{n}}_m$, $\tau_m = t - r_m/c$, $\tau_c = t - r_c/c$, $\tau_n = t - r_n/c$. The superscript † denotes a transpose.

It can be seen that there are eight terms in Eq. (20), and each term has three convolutions. Corresponding to three convolutions, the calculation of each term can be divided into three steps: aggregation; translation; disaggregation. It achieves the separation of the mth dipole and the nth dipole. Compared with the PWTD algorithm, the aggregation, translation and disaggregation processes do not require the calculation of the spherical Bessel functions, the Legendre polynomial and spherical integration, so it is relatively easy to implement. The aggregation-translation-disaggregation process will be detailed in the next subsection.

3.2. Computational Cost and Complexity

The preceding subsection outlined the procedure of the TD-FDM scheme. In this subsection, we further investigate the detail of TD-FDM and analyze its theoretical computational complexity and memory requirement. Assume that there are N_g nonempty groups, each containing approximately $M_s = N_s/N_g$ unknowns. In order to implement TD-FDM, first appropriate subsignal duration must be defined. The fundamental subsignal duration T_s is defined as

$$T_s = M_t \Delta t = \left(\left\lfloor \frac{\beta D}{c\Delta t} \right\rfloor - 1 \right) \Delta t. \tag{21}$$

This is because the field has been constructed via the three convolutions for the closest interaction of far-field pair.

After T_s has been defined, the TD-FDM for the fast evaluation of the sum on the RHS of Eq. (5) is divided into 4 steps: near-field evaluation, aggregation, translation and disaggregation. In what follows, implementation dependent constants are denoted as α_1–α_4. For the simplicity of discussion, we only consider the first term of Eq. (20) as an example to illustrate how the TD-FDM works.

(1) Near-field evaluation: At each time step, the sum

$$\sum_{j=0}^{i-1} \mathbf{Z}_{i-j}^{\alpha,\alpha'} I_j^{\alpha'}, \tag{22}$$

is computed for all near-field group pairs (α, α'). $\mathbf{Z}_{i-j}^{\alpha,\alpha'}$ denotes the submatrix of $\mathbf{Z}_{i-j}$. Assuming every group has N_p groups in its near region, the total number of groups need to be calculated and associated with near region interaction is $N_g N_p$. And there are M_s^2 impedance elements needed to be calculated in each group pair. The cost of all near-field interactions for all N_t time step is

$$T_1 = \alpha_1 N_g N_p M_s^2 N_t \approx \alpha_1 N_s^2 N_t / N_g. \tag{23}$$

(2) Aggregation: For each far-field pair, outgoing rays $V_1(t)$ generated by subsignals of the duration T_s are constructed every M_t time steps. This contribution aggregating the signal from the nth equivalent dipole to the group center O_i can be obtained by the rightmost convolution of Eq. (20)

$$V_1(t) = [\mathbf{m}_n \delta(t - r_n/c)] * I_{n,l}(t). \tag{24}$$

Constructing outgoing rays involves the aggregation of all current elements in the nonempty group pair for all N_t time steps. Since each group has $N_g - N_p$ groups in its far-field region, there are $N_g(N_g - N_p)$

far-field group pairs and each pair needs M_s operations. The cost of computing all aggregation is

$$T_2 = \alpha_2 N_g (N_g - N_p) M_s N_t \approx \alpha_2 N_g N_s N_t. \tag{25}$$

(3) Translation: Once outgoing rays $V_1(t)$ aggregated for each far-field pair, outgoing rays are immediately translated from the group center O_i to the group center O_j. Each outgoing ray is converted to an incoming ray by the middle convolution of Eq. (20)

$$V_2(t) = \left[\frac{1}{r_c^3}\delta(t - r_c/c)\right] * V_1(t), \tag{26}$$

where $\frac{1}{r_c^3}\delta(t - r_c/c)$ is termed the translation operator, and $V_2(t)$ represents incoming rays. The translation operator is nothing but a time delay temporally. Apparently, an outgoing ray requires one translation operation for a far-field group pair, so the cost of computing all translation is

$$T_3 = \alpha_3 N_g (N_g - N_p) N_t \approx \alpha_3 N_g^2 N_t. \tag{27}$$

(4) Disaggregation: Finally at each time step, the field at the observer can be formed by the left convolution of Eq. (20)

$$V_3(t) = \left[x_m^{(3)}(\mathbf{m}'_m \times \mathbf{R}_m)\delta(t - r_m/c)\right]^{\dagger} * \ V_2(t). \tag{28}$$

This process disaggregates the incoming rays from the the group center O_j to the mth equivalent dipole. This process involves a very similar operation to the aggregation process. Hence, the cost of computing all disaggregation is

$$T_4 = \alpha_4 N_g (N_g - N_p) M_s N_t \approx \alpha_4 N_g N_s N_t. \tag{29}$$

From the above discussion, the total computational cost associated with the TD-FDM is

$$T_{\text{total}} = T_1 + T_2 + T_3 + T_4. \tag{30}$$

The computational cost is minimized by choosing N_g proportional to $\sqrt{N_s}$. With this choice, the computational complexity of using the TD-FDM is of order $O(N_s^{3/2} N_t)$. The TD-FDM has the less computational complexity than the MOT method $O(N_s^2 N_t)$.

One thing in the above description of the proposed scheme should be worth pointing out. The time variable t was assumed to be continuous. In the practical scheme, time is discretized by time step Δt. In far-field evaluation, there are three temporal convolutions. Each convolution operation is nothing but a time shift. These convolutions do not require using fast Fourier transforms and it can be carried out in the time domain.

In the memory requirement aspect, the TD-FDM only needs to store the impedance elements of near region. For far field analysis, the storage of the translation operator is not necessary in TD-FDM. Furthermore, because once the outgoing ray finished aggregation, it immediately performs translation and disaggregation, TD-FDM needs not to store outgoing rays and incoming rays for different groups. Therefore, it requires less memory than the MOT method.

4. NUMERICAL RESULTS

This section provides several numerical results that serve both to validate the TD-FDM and to demonstrate its efficiency. All simulations are performed on a shared memory workstation equipped with Intel(R) Xeon(R) Dual CPU W5580 3.2 GHz (only one core is used) and 28 GB of RAM. In our implementation, we use the generalized minimal residual (GMRES) iterative solver for each time step and choose the identical residual error $\leq 10^{-6}$. The temporal basic function $T(t)$ is constructed using third order Lagrange interpolation [22]. The threshold of TD-FDM is chosen $\beta = 1$. The larger β is, the more costly and accurate the TD-FDM becomes.

In the first example, we consider a shallow cube with dimension

Table 1. Comparison of CPU time and memory cost.

Method	CPU Time	RAM
MOT	18 m20 s	2 GB
TD-FDM	6 m46 s	458 MB

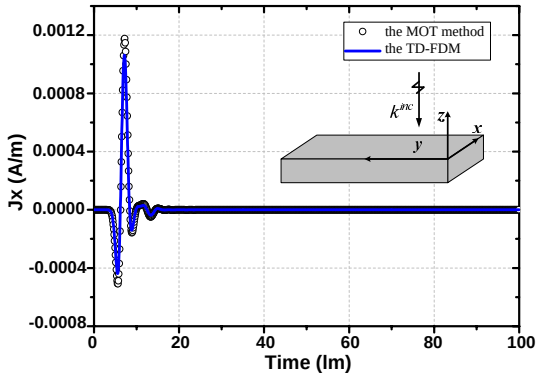

Figure 3. The current density at (0 m, 0 m, 0 m).

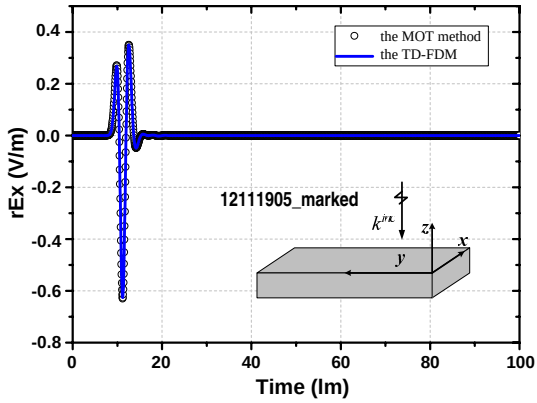

Figure 4. Back-scattered far field response.

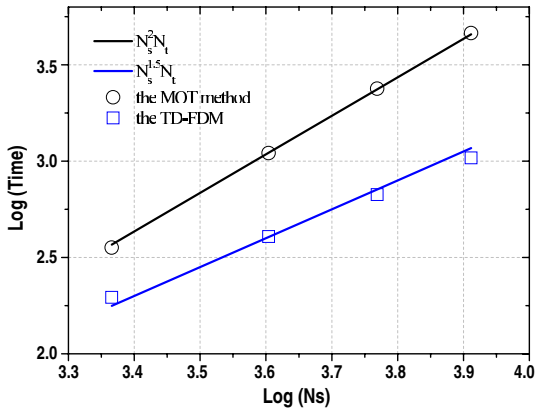

Figure 5. Comparison of the computational complexity.

$1.0\,\mathrm{m}\times 6.0\,\mathrm{m}\times 0.1\,\mathrm{m}$. The surface of the scatterer is discretized in terms of 4020 RWG basis functions. The incident wave is a Gaussian plane wave parameterized as $\mathbf{E}^i(\mathbf{r},t)=\hat{\mathbf{p}}\frac{4}{T_0\sqrt{\pi}}\exp[-\frac{16}{T_0^2}(ct-ct_0-\mathbf{r}\cdot\hat{\mathbf{k}})^2]$. Here $T_0=4\,\mathrm{lm}$ is the pulsewidth of the Gaussian impulse, $ct_0=6\,\mathrm{lm}$ is the time delay, $\hat{\mathbf{k}}=-\hat{\mathbf{z}}$ denotes the travel direction of the incident wave, and $\hat{\mathbf{p}}=-\hat{\mathbf{x}}$ is a unit vector of its polarization. The size of each group is 0.4 m, the time step size is 166.6 ps, and $N_t=2000$. Both CPU time and memory requirement of each method are listed in Table 1. The current density for x direction observed at the point (0 m, 0 m, 0 m) computed using both the TD-FDM and the MOT schemes are compared in Fig. 3. The back-scattered far field signal for x direction are compared in Fig. 4. The results are in good agreement with each

other. Furthermore, we fix N_t and discretize the shallow cube with different number of unknowns. Fig. 5 shows the computational time using the two methods for varying N_s. With N_s and N_t increasing, the classical MOT scheme will cost more CPU time and memory, so the following simulations are compared against the results computed using the frequency algorithm.

Next, transient scattering from a sphere of diameter 4 m is analyzed. The surface of the sphere is discretized using 18447 RWG basis functions. The incident wave is a Gaussian pulse with $\hat{\mathbf{p}} = -\hat{\mathbf{x}}$, $\hat{\mathbf{k}} = -\hat{\mathbf{z}}$, $T_0 = 2\,\mathrm{lm}$, and $ct_0 = 6\,\mathrm{lm}$. The size of each group is 0.35 m, $\Delta t = 133.3\,\mathrm{ps}$, and $N_t = 3000$. The temporal far-field signals

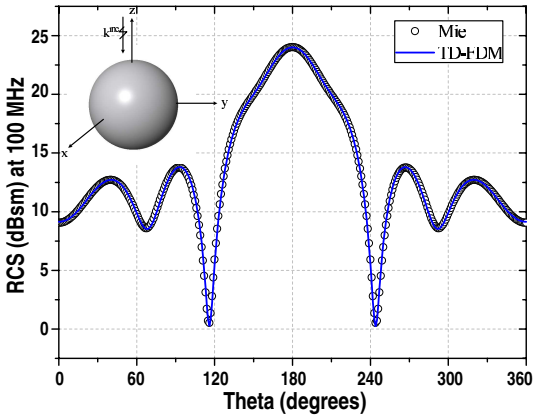

Figure 6. Comparison of the bistatic RCS at 100 MHz.

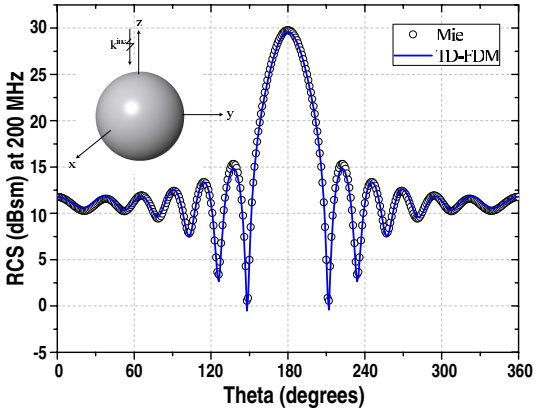

Figure 7. Comparison of the bistatic RCS at 200 MHz.

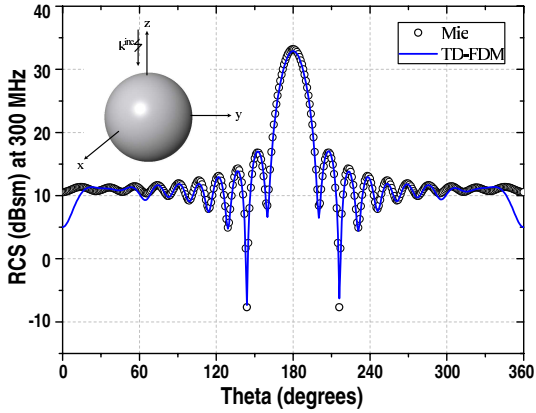

Figure 8. Comparison of the bistatic RCS at 300 MHz.

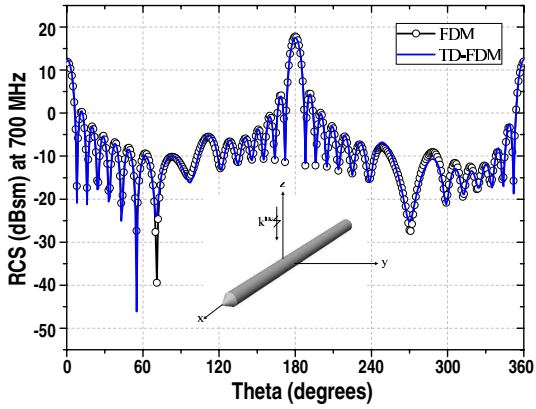

Figure 9. Comparison of the bistatic RCS at 700 MHz.

are Fourier transformed into the frequency domain. The bistatic radar cross-section (RCS) patterns computed using the TD-FDM are compared with the Mie method. The RCS was computed for $\phi = 0°$, and θ between 0° and 360°. Figs. 6–8 show the RCS patterns of the sphere at 100 MHz, 200 MHz, and 300 MHz. At 300 MHz, the power of the incident wave become relatively small. The results agree well with each other.

Finally, to further verify the validity of the TD-FDM, scattering from a PEC pencil target is analyzed. The pencil consisted of a 3 m long cylinder with radius 0.1 m, and a tip extending 0.173 m pointing toward $+x$ direction. The object is discretized into 31947 RWG basis functions. The incident wave is a modulated Gaussian plane wave parameterized as $\mathbf{E}^i(\mathbf{r},t) = \hat{\mathbf{p}} \exp[-\frac{1}{2\sigma^2}(\tau_0 - 8\sigma)^2] \cos(2\pi f_0 \tau_0)$. Here

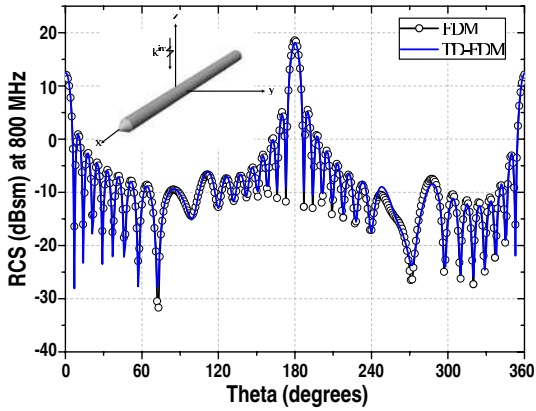

Figure 10. Comparison of the bistatic RCS at 800 MHz.

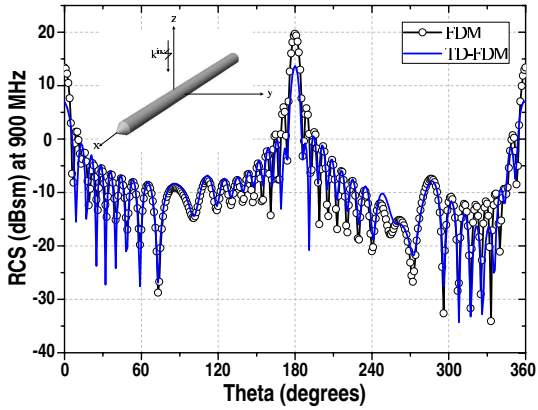

Figure 11. Comparison of the bistatic RCS at 900 MHz.

$f_0 = 800$ MHz is the center frequency, $f_{bw} = 300$ MHz is the bandwidth of the signal, $\sigma = 6/(2\pi f_{bw})$, and $\tau_0 = t - \mathbf{r} \cdot \hat{\mathbf{k}}/c$. The size of each group is 0.09 m, the time step size is 50 ps, and $N_t = 8000$. The RCS was computed for $\phi = 0°$, and θ between 0° and 360°. The bistatic RCS patterns at 700 MHz, 800 MHz, and 900 MHz obtained by the TD-FDM agree well with the FDM as shown in Figs. 9–11.

5. CONCLUSIONS

In this paper, the TD-FDM is proposed to accelerate the matrix-vector products in TDMFIE. The computational complexity of TD-FDM scales as $O(N_s^{3/2} N_t)$ as opposed to $O(N_s^2 N_t)$ for the MOT method.

The method is applied to compute the electromagnetic scattering from the PEC targets and numerical results demonstrate the validity and efficiency of our method. In our future work, the TD-FDM will be extended to the multilevel and the computational complexity will be further reduced.

ACKNOWLEDGMENT

This work is supported by the National Natural Science Foundation of China under Grant No. 61071019, the National Natural Science Foundation of China for Young Scholars under Grant No. 61102033, the Fundamental Research Funds for the Central Universities under Grant NS2012096 and the Foundation of State Key Laboratory of Millimeter Waves, Southeast University, P. R. China under Grant No. K201302.

REFERENCES

1. Rao, S. M. and D. R. Wilton, "Transient scattering by conducting surfaces of arbitrary shape," *IEEE Trans. Antennas Propagat.*, Vol. 39, No. 1, 56–61, Jan. 1991.
2. Shanker, B., A. A. Ergin, K. Aygun, and E. Michielssen, "Analysis of transient electromagnetic scattering from closed surfaces using a combined field integral equation," *IEEE Trans. Antennas Propagat.*, Vol. 48, No. 7, 1064–1074, Jul. 2000.
3. Jung, B. H., Z. Mei, and T. K. Sarkar, "Transient wave propagation in a general dispersive media using the Laguerre function in a marching-on-in-degree (MOD) methodology," *Progress In Electromagnetics Research*, Vol. 118, 135–149, 2011.
4. Zhu, H., Z.-H. Wu, X. Y. Zhang, and B.-J. Hu, "Time-domain integral equation solver for radiation from dipole antenna loaded with general bi-isotropic objects," *Progress In Electromagnetics Research B*, Vol. 35, 349–367, 2011.
5. Luo, W., W. Y. Yin, M. D. Zhu, and J. Y. Zhao, "Hybrid TDIE-TDPO method for studying on transient responses of some wire and surface structures illuminated by an electromagnetic pulse," *Progress In Electromagnetics Research*, Vol. 116, 203–219, 2011.
6. Zhu, M. D., X. L. Zhou, W. Luo, and W. Y. Yin, "Hybrid TDIE-TDPO method using weighted laguerre polynomials for solving transient electromagnetic problems," *Progress In Electromagnetics Research*, Vol. 126, 375–398, 2012.
7. Sirenko, K., V. Pazynin, Y. K. Sirenko, and H. Bağci, "An FFT-accelerated FDTD scheme with exact absorbing conditions for

characterizing axially symmetric resonant structures," *Progress In Electromagnetics Research*, Vol. 111, 331–364, 2011.

8. Wang, J.-B., B.-H. Zhou, L.-H. Shi, C. Gao, and B. Chen, "A novel 3-D weakly conditionally stable FDTD algorithm," *Progress In Electromagnetics Research*, Vol. 130, 525–540, 2012.
9. Ergin, A. A., B. Shanker, and E. Michielssen, "The plane wave time-domain algorithm for the fast analysis of transient wave phenomena," *IEEE Antennas Propagat. Mag.*, Vol. 41, No. 4, 39–52, Sept. 1999.
10. Shanker, B., A. A. Ergin, K. Aygun, and E. Michielssen, "Analysis of transient electromagnetic scattering phenomena using a two-level plane wave time domain algorithm," *IEEE Trans. Antennas Propagat.*, Vol. 48, No. 4, 510–523, Apr. 2000.
11. Shanker, B., A. A. Ergin, M. Y. Lu, and E. Michielssen, "Fast analysis of transient electromagnetic scattering phenomena using the multilevel plane wave time domain algorithm," *IEEE Trans. Antennas Propagat.*, Vol. 51, No. 3, 628–641, Mar. 2003.
12. Yilmaz, A. E., J. M. Jin, and E. Michielssen, "Time domain adaptive integral method for surface integral equations," *IEEE Trans. Antennas Propagat.*, Vol. 52, No. 10, 2692–2708, Oct. 2004.
13. Yilmaz, A. E., J. M. Jin, and E. Michielssen, "Analysis of low-frequency electromagnetic transients by an extended time-domain adaptive integral method," *IEEE Trans. Advanced Packaging*, Vol. 30, No. 2, 301–312, May 2007.
14. Garcia, E., C. Delgado, L. Lozano, I. Gonzalez-Diego, and M. F. Catedra, "An efficient hybrid-scheme combining the characteristic basis function method and the multilevel fast multipole algorithm for solving bistatic RCS and radiation problems," *Progress In Electromagnetics Research B*, Vol. 34, 327–343, 2011.
15. Wang, W. and N. Nishimura, "Calculation of shape derivatives with periodic fast multipole method with application to shape optimization of metamaterials," *Progress In Electromagnetics Research*, Vol. 127, 49–64, 2012.
16. Ding, J., C. Gu, Z. Niu, and Z. Li, "Application of the equivalent dipole moment method for transient electromagnetic scattering," *International Conference on Microwave and Millimeter Wave Technology, ICMMT Proceedings*, Vol. 3, 898–900, 2012.
17. Chen, X., C. Gu, Z. Niu, and Z. Li, "Fast dipole method for electromagnetic scattering from perfect electric conducting targets," *IEEE Trans. Antennas Propagat.*, Vol. 60, No. 2, 1186–1191, Feb. 2012.

18. Chen, X., C. Gu, Z. Niu, and Z. Li, "Reply to "Comments on 'Fast dipole method for electromagnetic scattering from perfect electric conducting targets'"," *IEEE Trans. Antennas Propagat.*, Vol. 60, No. 12, 6063–6064, Dec. 2012.
19. Chen, X., Z. Li, Z. Niu, and C. Gu, "Analysis of electromagnetic scattering from PEC targets using improved fast dipole method," *Journal of Electromagnetic Waves and Applications*, Vol. 25, No. 6, 2254–2263, 2012.
20. Ergul, O. and L. Gurel, "The use of curl-conforming basis functions for the magnetic-field integral equation," *IEEE Trans. Antennas Propagat.*, Vol. 54, No. 7, 1917–1926, Jul. 2006.
21. Yuan, J., C. Gu, and G. Han, "Efficient generation of method of moments matrices using equivalent dipole-moment method," *IEEE Antennas Wireless Propagat. Lett.*, Vol. 8, 716–719, 2009.
22. Aygun, K., M. Lu, B. Shanker, and E. Michielssen, "Analysis of PCB level EMI phenomena using an adaptive low-frequency plane wave time domain algorithm," *IEEE International Symposium on Electromagnetic Compatibility*, Vol. 1, 295–300, 2000.